Environ Biol Fish (2007) 80:293–308
DOI 10.1007/s10641-007-9220-y

SPECIAL ISSUE SKATES

Age and growth estimates for the smooth skate, *Malacoraja senta*, in the Gulf of Maine

Lisa J. Natanson · James A. Sulikowski · Jeff R. Kneebone · Paul C. Tsang

Received: 10 July 2006 / Accepted: 11 January 2007 / Published online: 21 February 2007

Abstract Age and growth estimates for the smooth skate, *Malacoraja senta*, were derived from 306 vertebral centra from skates caught in the North Atlantic off the coast of New Hampshire and Massachusetts, USA. Males and females were aged to 15 and 14 years, respectively. Male and female growth diverged at both ends of the data range and the sexes required different growth functions to describe them. Males followed a traditional growth scenario and were best described by a von Bertalanffy curve with a set L_o (11 cm TL) where L_{inf} = 75.4 cm TL, K = 0.12. Females required the use of back-calculated values to account for a lack of small individuals, using these data they were best described by a von Bertalanffy curve where growth parameters derived from vertebral length-at-age data are L_{inf} = 69.6 cm TL, K = 0.12, and L_o = 10.

Keywords Vertebra · Skate · Age

L. J. Natanson (✉)
USDOC/NOAA/NMFS, 28 Tarzwell Drive,
Narragansett, RI 02882, USA
e-mail: Lisa.Natanson@noaa.gov

J. A. Sulikowski
Marine Science Center, University of New England,
Biddeford, ME 04005, USA

J. R. Kneebone · P. C. Tsang
Animal and Nutritional Sciences, University of New
Hampshire, Durham, NH 03824, USA

Introduction

The smooth skate, *Malacoraja senta*, is one of the smallest (<70 cm total length; <2.0 kg wet weight) species of skate endemic to the western North Atlantic Ocean (McEachran 2002). *M. senta* has a relatively broad geographic distribution, ranging from Newfoundland and southern Gulf of St. Lawrence in Canada to New Jersey in the United States (Robins and Ray 1986; McEachran 2002), yet the only direct biological data for this species pertains to the reproductive cycle for specimens in the Gulf of Maine (Sulikowski et al. in press). Although no directed fisheries for this species exist in the Gulf of Maine, this skate is taken as bycatch (New England Fishery Management Council [NEFMC] 2001).

The vulnerability of sharks to exploitation as bycatch in commercial fisheries is well documented (Bonfil 1994; Musick 1999, 2004). However, recent population assessments of skates suggest these elasmobranchs are also at risk. For example, Dulvy and Reynolds (2002) recently confirmed the disappearance of the common skate, *Dipturus batis*, from the Irish Sea, and reported that the long nose skate, *D. oxyrhinchus* and the white skate, *Rostroraja alba*, were also absent from substantial parts of their ranges. In the western North Atlantic, there have been declines in barndoor, *Dipturus laevis* (Casey and

Meyers 1998), thorny, *Amblyraja radiata*, and smooth skate, stocks (NEFMC 2001, 2003). As a result of these circumstances, commercial landing of these three species is now prohibited in the Gulf of Maine (NEFMC 2003). However, these species continue to suffer the threat of population decline through the indirect fishing pressures of bycatch mortality.

Age information forms the basis for the calculations of growth rate, mortality rate and productivity, making it one of the most influential variables for estimating a population's status and assessing the risks associated with exploitation. Given the current predicament of *M. senta* stocks in the Gulf of Maine, the objective of the present study was to establish age and growth rates of *M. senta* based on annular bands counts within the vertebral centra.

Materials and methods

Collection

Smooth skates were captured 30–40 km off the coast of New Hampshire and Massachusetts, USA, by otter trawl in an approximate 2,300 square km area centered at 42° 50′ N and 70° 15′ W in the Gulf of Maine. Skates were maintained alive on board the F/V Mystique Lady until transport to the University of New Hampshire's Coastal Marine Laboratory (CML). There, individual fish were euthanized (0.3 $g \cdot l^{-1}$ bath of MS222) and morphological measurements, such as total length (TL in cm), disk width (DW in cm), and total wet weight (kg) were recorded. A block of 10 vertebrae from above the abdominal cavity was removed from smooth skates, labeled, and stored frozen. Vertebrae sent for histology were stored in ethanol for transport.

Histology—To ensure an adequate number of sections, two whole vertebrae from each sample were processed for histology. Standard techniques for calcified tissues were adjusted based on the size of the vertebrae (Humason 1972). As per Casey et al. (1985) *tert*-butyl alcohol was used in place of xylene during infiltration to eliminate hardening and distortion of the calcified tissue. Vertebrae were removed from ethanol, and placed in individual tissue capsules. Samples of similar size were decalcified together in a large beaker filled with 100% RDO® rapid decalcifying agent. Constant movement of the solution was provided by a mixing plate and magnetic stir-bar. The length of decalcification varied between a 30 min and 4 h depending on the size of the centrum. The stage of decalcification was determined by the ease with which a sharp scalpel could trim off a section of the vertebra. Once the blade could easily pass through the vertebra with no signs of calcification, decalcification was considered complete. Centra were then transferred to a beaker of running water for several hours. Decalcified centra were stored in 70% ethanol until processing.

Vertebrae were embedded using a nine-step process with each lasting for 2 h (Table 1a). At the completion of step nine, vertebrae were immediately placed in embedding molds filled with 100% Paraplast Plus®. One vertebra of the two processed from each specimen was sectioned, while the other was used as a spare. The embedded centra were sectioned with a sledge microtome to obtain 80–100 μm sections from the center of the centra. The focus of the section was determined by the presence of the notochordal remnant. One to eight sections were obtained from each sample. Sections were placed by sample into a tissue capsule and temporarily immersed in 100% xylene. Paraplast Plus® was progressively removed from the sections in preparation for staining (Table 1b). Once stained with Harris hematoxylin, the sections were brought into glycerin in preparation for mounting on microscope slides with Kaiser Glycerin Jelly (Table 1b). Lastly, the sections were sealed with clear nail polish (Humason 1972).

Each section was digitally photographed with an MTI CCD 72 video camera attached to a SZX9 Olympus stereomicroscope[1] using reflected light and a white background. Band pairs (consisting of one opaque and one translucent band) were counted and measured on the images using Image Pro 4 software. Measurements were made from the midpoint of the notochordal remnant (focus)

[1] Reference to trade names does not imply endorsement by the National Marine Fisheries Service.

Table 1 Embedding procedure and Staining procedure

Step	Percent alcohol	Formula	Time (h)	Temperature
(a) Embedding procedure				
1	70%	500 ml ethanol 300 ml distilled water 200 ml *tert*-butyl alcohol	2	Room
2	85%	500 ml ethanol 150 ml distilled water 350 ml *tert*-butyl alcohol	2	Room
3	100%	450 ml ethanol 550 ml *tert*-butyl alcohol	2	Room
4	100%	250 ml ethanol 750 ml *tert*-butyl alcohol	2	Room
5	100%	1000 ml *tert*-butyl alcohol	2	Room (warm enough to be liquid)
6	100%	1000 ml *tert*-butyl alcohol	2	Room (warm enough to be liquid)
7	50%	500 ml *tert*-butyl alcohol 500 ml Paraplast Plus®	2	60°F
8		1000 ml Paraplast Plus®	2	60°F
9		1000 ml Paraplast Plus®	2	60°F

Step	Formula	Time (min)	Notes
(b) Staining procedure			
1	100% xylene	3–10	Time in xylene depends on amount of Paraplast Plus® in tissue and size of tissue. Increase time for increased Paraplast Plus® and tissue size.
2	100% xylene	3–10	
3	100% xylene	3–10	
4	100% ethanol	5	
5	100% ethanol	5	
6	100% ethanol	5	
7	95% ethanol 5% distilled water	5	
8	80% ethanol 20% distilled water	5	
9	100% distilled water	5	Process can be stopped here for overnight
10	Harris Hematoxylin	10	Sections should be checked to ensure proper staining
11	Water rinse	until clear	

Table 1 continued

Step	Formula	Time (min)	Notes
(b) Staining procedure			
12	Acid alcohol*	2	This can be adjusted depending on staining strength
13	Water rinse	1	Use agitation
14	Lithium carbonate**	5	or until the tissue turns blue
15	Running water	10	
16	Distilled water	2	
17	25% glycerin	10	
18	50% glycerin	10	
19	75% glycerin	10	
20	100% glycerin	10	Tissues can be stored for longer periods at this step

* Acid alcohol—65% distilled water, 35% ethanol, 6 drops hydrochloric acid per 100 ml

** Lithium carbonate—400 ml distilled water, 0.2 gm lithium carbonate

of the full bow tie to the opaque growth bands at points along the internal corpus calcareum. The radius of each centrum (VR) was measured from the midpoint of the notochordal remnant to the distal margin of the intermedialia along the same diagonal as the band measurements.

The relationship between VR and TL was calculated to determine the best method for back-calculation of size at age data and to confirm the interpretation of the birth band. Regressions were fit to the male and female data and an ANCOVA was used to test for difference between the two relationships. The relationship between TL and VR was best described by a quadratic equation; therefore the data were ln-transformed before linear regression. The quadratic-modified Dahl-Lea was used for back calculation:

$$L_i = L_c * [(a + bVR_i + cVR_i^2)/(a + bVR_c + cVR_c^2)] \quad (1)$$

where a, b and c are the quadratic fit parameter estimates; VR_i = vertebral radius at band "i"; and VR_c = vertebral radius at capture. Due to a lack of small individuals back-calculations were performed on both sexes.

Vertebral centrum interpretation

A band pair consisted of one opaque and one translucent band. The criteria for designating a band pair were based on broad opaque and translucent bands, each of which was composed of layers of distinct thinner rings (sensu Cailliet et al. 1983; Martin and Cailliet 1988). In most cases the intermedialia was not present thus the bands were determined solely by their appearance on the corpus calcareum. Due to the consistency in counts between the corpus calcareum and intermedialia in those samples which had both we were confident that the counts from the corpus only were representative of the age.

Data analysis

Initial count comparison between co-authors was undertaken on the female sample. Ageing bias and precision of bands counts were examined using APE, D, (Beamish and Fournier 1981) and the coefficient of variation (CV) (Chang 1982). Additionally, a contingency table was made and Chi-square tests of symmetry (McNemar 1947; Bowker 1948; Hoeing et al. 1995; Evans and

Hoenig 1998) performed to determine whether differences between readers were biased or due to random error. An age-bias plot was also calculated (Campana et al. 1995).

Once the criteria for the bands were determined using the within reader comparison, reader 1 (JAS) counted the male sample set and reader 2 (JRK) counted the female sample set. Both sample sets were counted twice. Pairwise comparisons of precision and bias were conducted on the two counts for each sex. Samples that still did not agree were recounted, if a consensus was not reached at that time, the sample was discarded.

Von Bertalanffy growth functions (VBGF) were fit to observed total length-at-age data and back-calculated data using the original equation of von Bertalanffy (1938) with size at birth L_o rather than t_o:

$$L(t) = L_\infty - (L_\infty - L_o)exp^{-kt} \quad (2)$$

where $L(t)$ = predicted length at time t; L_∞ = mean asymptotic total length; k = a rate parameter (yr^{-1}); and L_o = total length at birth.

Two variations of the model were used: 3-parameter calculation estimated L_∞, k and L_o, 2-parameter method estimated L_∞ and k and incorporated a set L_o = 11 cm TL (Kulka and Sulikowski Unpub. data[2]).

As an alternative to the VBGF analysis, we used the Gompertz growth function (GGF) as described in Ricker (1979):

$$L(t) = L_0 e^{G(1-e^{(-kt)})} \quad (3)$$

where $L_\infty = L_o e^G$ is the mean maximum TL ($t = \infty$); k (= g in Ricker, 1975) is a rate constant (yr^{-1}), and L_o = total length at birth.

Two variations of this model were also fit to the data as above with unconstrained parameters and with L_o set using the same value as with the VBGF. All of these growth equations were fit using non-linear regression in Statgraphics (Manuguistics)® on both the observed length and back calculated at age data independently.

[2] Unpub. data. 2006. Kulka, D.W. Marine Fish Species at Risk, Fisheries and Oceans, Science, Aquatic Resources Northwest Atlantic Fisheries Centre, St Johns, Newfoundland & Labrador, A1C 5X1 Canada.

Additionally, we applied five cases of the Schnute (1981) growth model, as presented by Bishop et al. (2006), to the observed length at age data. The best fitting case was determined using Akaike's (1973) Information Criterion (AIC), and the Bayesian Information Criterions (BIC) using the following equations:

$$AIC = -2(LL) + 2p \quad (4)$$

where LL is the maximum log-likelihood for each model and p is the number of model parameters.

$$BIC = -2(LL) + p\ln(n) \quad (5)$$

where n = sample size.

Comparison of growth between the sexes

The Kimura (1980) method of using χ^2 tests on each likelihood ratio were used to compare the data between sexes for VBGF. Likelihood ratio and chi-square tests were performed in Microsoft Excel® as outlined by Haddon (2001). Additionally, the AIC and BIC of the best fitting Schnute (1981) case with sexes combined was compared the values for of sexes separate to determine if the sexes grew similarly.

Verification

The periodicity of band pair formation was investigated using marginal increment ratio (MIR) (Skomal 1990; Goldman 2004). The MIR was calculated as the ratio of the distance between the last band pair to the margin to the width of the last complete band pair. Average MIR was plotted by month of capture to identify trends in band formation, and a Kruskal-Wallis one-way analysis of variance on ranks was used to test for differences in marginal increment by month (Simpfendorfer et al. 2000).

Longevity

Three methods were used to estimate longevity. The oldest fish aged from the vertebral method provides an initial estimate of longevity; however, this value is likely to be underestimated in a

fished population as large individuals are removed from the fishery. Taylor (1958) defined the life span of a teleost species as the time required to attain 95% of L_∞. The estimated age at 95% of L_∞ (=longevity in years) was calculated by solving the VBGF and GGFs for t and replacing $L_{(t)}$ with $0.95L_\infty$. For the VBGF we obtained:

$$Longevity = (1/k)\ln\left[\frac{(L_\infty - L_0)}{L_\infty(1-x)}\right] \quad (6)$$

and for the Gompertz growth curves we obtained:

$$Longevity = (1/k)\ln\left[\frac{\ln(L_0/L_\infty)}{\ln(x)}\right] \quad (7)$$

where $x = L(t)/L_\infty = 0.95$.

Results

Vertebral samples from 405 smooth skates (189 males, 216 females) were processed. Poor slide quality (90) and/or lack of length data (10) reduced the readable sample size to 306 (153 males, 153 females). Samples ranged in size from 30.0 to 68.0 cm TL for males and 32.5–62.5 cm TL for females.

Vertebral centrum interpretation

The TL-VR data was best described as a polynomial for both sexes (Fig. 1). The data were log-transformed and fit with a linear regression to compare between the sexes. There was no significant difference between the sexes for intercept ($p = 0.719$) however, there was a significant difference in the slope ($p = 0.0010$).

Therefore, we calculated the quadratic regressions for sexes separately. The regressions were:

$$TL = -5.60 + 33.75*VR - 4.39*VR^2 \quad R^2 = 0.73,\ n = 146,\ female; \quad (8)$$

$$TL = -0.51 + 26.26*VR - 2.30*VR^2 \quad R^2 = 0.82,\ n = 144,\ male. \quad (9)$$

Smooth skate vertebrae did not show consistent pre-birth marks; thus, the first distinct opaque band was defined as the birth band. The location of the birth band (BB) was just outside of the focus there was no angle change associated with this mark (Fig. 2). The mean BB value was not significantly different between males and

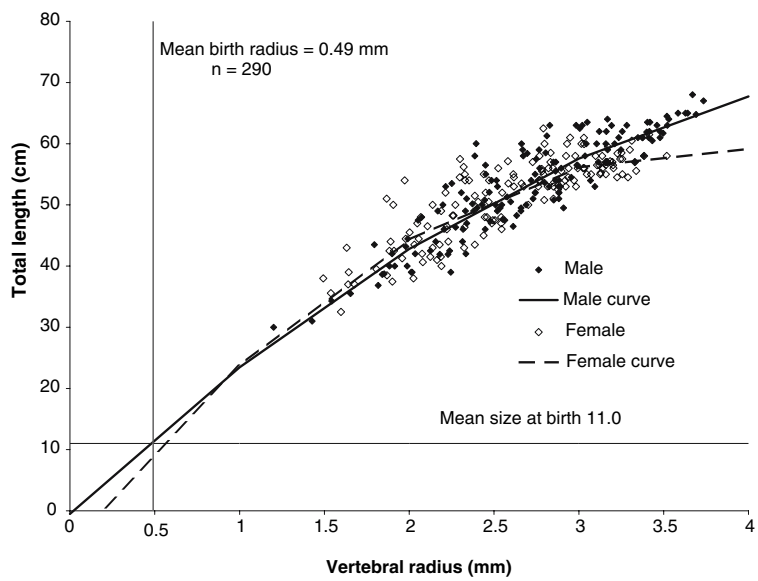

Fig. 1 Relationship between vertebral radius and total length for male and female smooth skates. The horizontal dotted line represents the size at birth and the vertical dotted line represents the mean radius of the birth mark

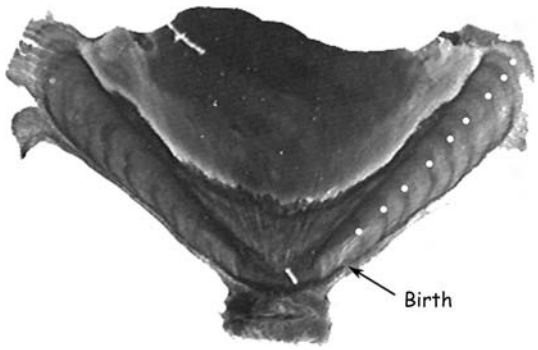

Fig. 2 Photograph of a vertebral section from a 50 cm TL male smooth skate estimated to be 9 years-old. The birth band (BB) is indicated and band pairs are marked with a light circle. Vertebral radius = 2.2 mm

females (Kolmogorov-Smirnov $p = 0.273$) and the sexes were combined for analysis. The mean BB value of the total sample was 0.49 mm ± 0.01 mm (±95% CI) ($N = 290$). Since the mesh size of the commercial trawl precluded the capture of young-of-the-year (YOY) to compare with this radius, we back calculated the lengths at BB for the entire sample using Eq. (1) to obtain an associated mean length at birth and ensure the BB was identified correctly. The calculated birth mean TL (10.84 cm ± 0.30 cm; $N = 290$) is very close to the 11 cm TL size at birth estimated for this species (Kulka and Sulikowski Unpub. data[2]).

Data analysis

Comparison of counts between readers indicated that all readers were identifying the same bands. The CV between Readers 1 and 2 ($n = 100$) varied about a mean of 4.3%. Age bias plots showed minimal variation around the 1:1 ratio and no systematic bias (Fig. 3a). Additionally, the Bowker (1948), McNemar (1947), Hoeing et al. (1995) Evans and Hoenig (1998) χ^2 tests of symmetry gave no indication that differences between readers were systematic rather than due to random error (χ^2 test, $p > 0.05$ in all cases).

Comparison of the first and second counts of each reader also indicated no systematic bias. The individual CV, APE and D were 1.52%, 1.16% and 1.08% for males (Reader 1; $N = 153$) and 5.54%, 5.88%, and 3.92% for females (Reader 2; $N = 153$) (Fig. 3b, c). In the absence of bias, the level of precision was considered acceptable.

Back-calculation

While the back-calculated values were slightly lower on average than the observed for both sexes (4.8% and 7.5% males and female, respectively), the majority of points overlapped and there was no evidence of Lee's Phenomenon (Fig. 4a, b). In the early portion of the female relationship the actual data are limited and do not fall to the known size at birth; the back-calculated data adequately fill in these size classes. Sizes estimated for birth (11.5 cm TL and 10.2 cm TL) were close to estimates of known values.

Growth rates

Male and female growth rates were significantly different (Kimura 1980, $\chi^2 = 36.75$; $p < 0.001$). Additionally, the AIC and BIC values from the best fitting Schnute case (2) were lower for the sexes separate than together, confirming a difference in growth rates between the sexes. Thus, growth models were fit separately by sex (Table 2). Using the assumption of annual band pair deposition, all of the growth curves were fitted to the observed length at age data, additionally the VBGF and the Gompertz models were fit to the back-calculated length at age data.

Male growth curves

All the growth curves fit the male observed data over the aged size ranges (Fig. 5a). The Schnute (1981) Case 2, which is basically a form of the GGF 3 parameter, was the best Case using the Schnute (1981) model. The Schnute (1981) Case 2 and GGF 3 curves were identical; and overestimated size at birth (Table 3 and Fig. 5a). The VBGF 2 and 3 parameter estimations were very similar and provided reasonable estimates of the parameters for males based on observed values of size at birth and maximum size. The residual sum of squares (RSS) (636.3) for the 2 parameter model indicate that this is a slightly better fit to the data.

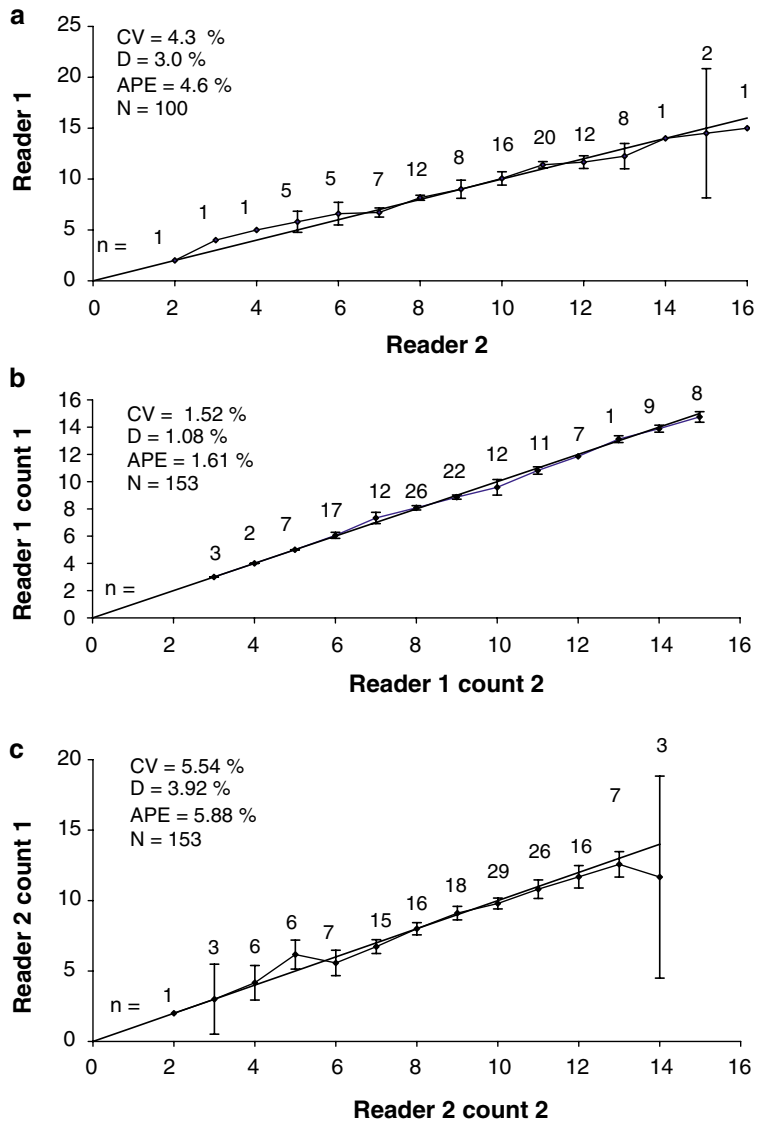

Fig. 3 Age bias graphs for pair-wise comparison of smooth skate vertebral counts from (**a**) two independent age readings by the one each by reader 1 and 2, $n = 100$; (**b**) two independent age readings by reader 1, $n = 153$; (**c**) two independent age readings by reader 2, $n = 153$. Each error bar represents the 95% confidence interval for the mean age assigned in reading 2 to all fish assigned a given age in reading 1. The one to one equivalence line is also presented as are the estimates of APE, D and CV

All the growth curves fit the male back-calculated data over the size range aged (Fig. 5b). The VBGF 3 parameter model provided the best fit (RSS = 9694.5) and provided reasonable estimates of the parameters for males based on observed values of size at birth and maximum size (Table 4). The fit of both the back-calculated VBGF 3 and the observed VBGF 2 are almost identical over the data (Fig. 5b, c). However, the L_∞ value is better represented in the observed VBGF 2 parameter model; thus, this model was chosen to represent the male growth in further analyses (Table 3).

Female growth curves

In contrast to the males, female observed growth was more difficult to define. As with the males, the Schnute (1981) Case 2 provided the best fit for the Schnute (1981) model and it was an identical curve to the GGF 3 parameter (Fig. 6a and Table 3). These two curves and the VBGF 3 parameter fit the data but overestimated the size at birth. These overestimates are probably due to a lack of small samples and the variability in those sampled. The VBGF and GGF models with the L_0 set provided good fits to the data at ages five to

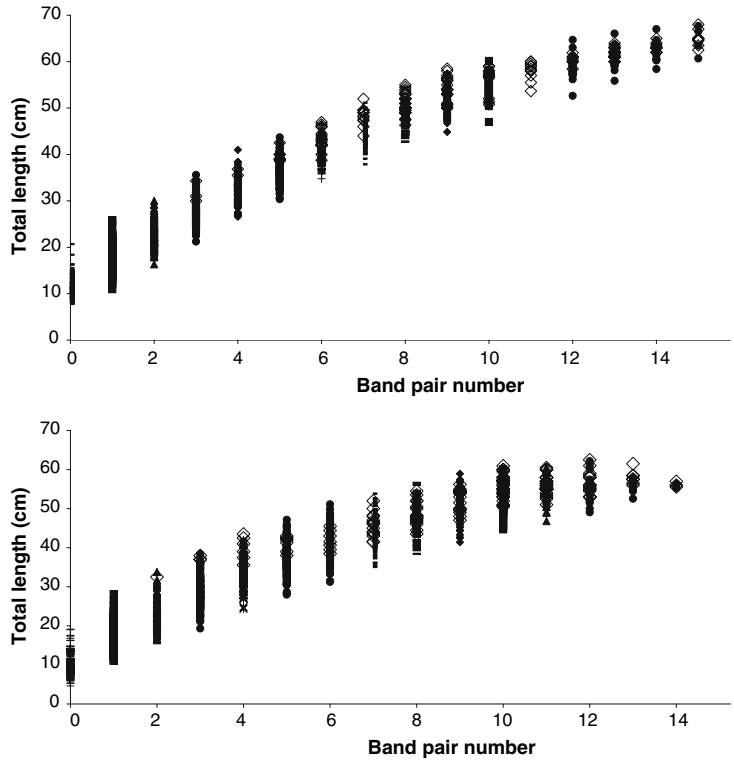

Fig. 4 Smooth skate band pair counts versus total length based on back-calculated data (solid symbols) and observed data (opened diamonds) of (**a**) males and (**b**) females

Table 2 Comparison of AIC and BIC for the Schnute case 2 model, for sexes combined and separate

Model	Sex	Growth function	N	RSS	Log likelihood	# params	AIC	BIC
1b	Combined	Schnute 2	305	2287	–740.02	4	1488.05	1502.93
2	Males	Schnute 2	153	629	–356.95			
2	Females	Schnute 2	152	1269	–354.62			
2	Separately	Schnute 2	305	1898	–711.57	7	1437.13	1463.18

14. Despite the high L_o, the comparison of RSS suggest that the GGF 3 model provided the best fit to the data.

All the growth curves fit the female back-calculated data over the size range aged (Fig. 6b and Table 4). The VBGF 3 parameter model provided the best fit (RSS = 18065.6) and reasonable estimates of the parameters for females based on observed values of size at birth and maximum size. The lower portion of the curve of the back-calculated VBGF 3 is more reasonable than that of the best fitting observed model (GGF 3 parameter, $R^2 = 80.2$) (based on observed values of size at birth and maximum size) and warrants the use of the back-calculated VBGF 3 model for the females. The L_∞ and K parameter estimations for both models are similar; the difference between the models lies in the estimations of L_0 which is improved by filling in the lower portion of the curve with the back-calculated values. The curves are similar after age 6, prior to this age they are effected by the different size at birth estimations (Fig. 6c). Due to the similarity between the back calculated and observed data, and the lack of any Lee's phenomenon, we feel that our results accurately represent growth rates of female smooth skates. Thus, the back-calculated VBGF 3 parameter estimation was chosen to represent the female growth rates in further analyses (Table 4).

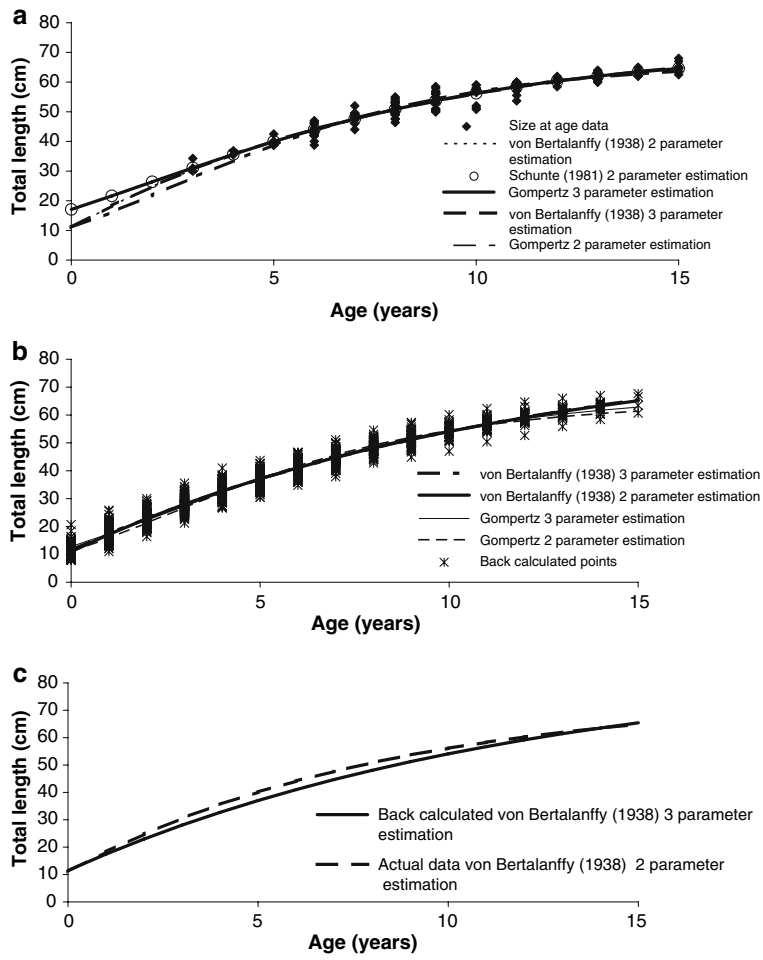

Fig. 5 Male smooth skate growth curves based on (**a**) observed data; (**b**) back-calculated data; and (**c**) observed and back-calculated comparison

Verification

Marginal increment analyses were performed on 120 female and 131 male skates over the range of age and size classes. In males, marginal increments were significantly different between months (Kruskal-Wallis $p < 0.001$); with a distinct trend of increasing monthly increment growth peaking in July, followed by a decline then nadir in December (Fig. 7a). Based on this information, the increment analyses support the likelihood that a single opaque band may be formed annually on male vertebral centra during December. Although an increasing trend that peaked in October was present in female marginal increments, these values were not significantly different between months (Kruskal-Wallis $p = 0.081$; Fig. 7b). Thus, in contrast to males, the periodicity of annual band formation in females lacks statistical verification.

Longevity

The maximum age based on vertebral band pair counts was 15 and 14 years, for males and females, respectively. The calculated longevity estimates using the values appropriate for each sex are 24 years for males and 23 years for females.

Discussion

The histological processing of smooth skate vertebrae resulted in the elucidation of alternating opaque and translucent bands. Using this method,

Table 3 von Bertalanffy growth function parameters and 95% confidence intervals calculated by using observed vertebral counts

Method		L_{inf}	K	L_0	n	Longevity	Residual sum of squares
von Bertalanffy—3 parameter	Male	75.487	0.120	11.041	153	23.6	636.3
	CI±	4.523	0.025	5.069			
	Female	74.970	0.090	22.657	152	31.4	1289.4
	CI±	14.225	0.051	5.810			
von Bertalanffy—2 parameter	Male	75.456	0.120		153	23.6	636.3
	CI±	2.415	0.009				
	Female	63.762	0.170		152	16.5	1409.2
	CI±	2.614	0.021				
Gompertz—3 parameter	Male	70.857	0.182	17.080	153	18.3	629.1
	CI±		0.027	2.857			
	Female	68.402	0.145	24.228	152	20.7	1268.7
	CI±		0.054	4.323			
Gompertz—2 parameter	Male	66.888	0.240		153	14.9	710.3
	CI±		0.009				
	Female	59.184	0.298		152	11.7	1625.9
	CI±		0.022				

vertebral sections were easy to interpret, and false bands (those bands that did not completely encircle the centra) were easily distinguished from complete bands. Precision and lack of bias in our estimates suggest that our band interpretation methods represent a precise approach for ageing *M. senta.*

While we are confident in our ability to determine band pairs with consistency, we are lacking accuracy, as we have no validation of the periodicity of band pair formation. The Kruskal-Wallis test indicated that there was a significant difference in the monthly MIR in males, however, the female result, though very close to significant at ($p = 0.08$) was not. Yoccoz (1991) suggested that biological significance cannot always be related to statistical significance and in the current case we believe this argument is substantiated. In female smooth skates there are clear transitional peaks and numerical lows observed in the monthly MIR. Moreover, the 0.08 p-value was very close to statistical significant level set at 0.05, which suggests that, while not statistically significant, a biologically important event was occurring in female vertebrae.

Table 4 von Bertalanffy growth function parameters and 95% confidence intervals calculated by using back-calculated vertebral counts

Method		L_{inf}	K	L_0	n	Longevity	Residual sum of squares
von Bertalanffy—3 parameter	Male	88.037	0.081	11.478	1493	35.2	9694.5
	CI±	3.005	0.005	0.320			
	Female	69.606	0.125	10.021	1479	22.5	18065.6
	CI±	2.235	0.009	0.462			
von Bertalanffy—2 parameter	Male	85.756	0.086		1493	33.3	9750.4
	CI±	2.312	0.004				
	Female	72.156	0.114		1479	24.8	18280.4
	CI±	2.283	0.007				
Gompertz—3 parameter	Male	68.273	0.200	12.806	1493	17.4	10181.7
	CI±		0.006	0.278			
	Female	58.991	0.263	11.400	1479	13.2	18489.1
	CI±		0.011	0.397			
Gompertz—2 parameter	Male	64.809	0.232		1493	15.2	11305.8
	CI±		0.004				
	Female	58.460	0.272		1479	12.8	18539.6
	CI±		0.007				

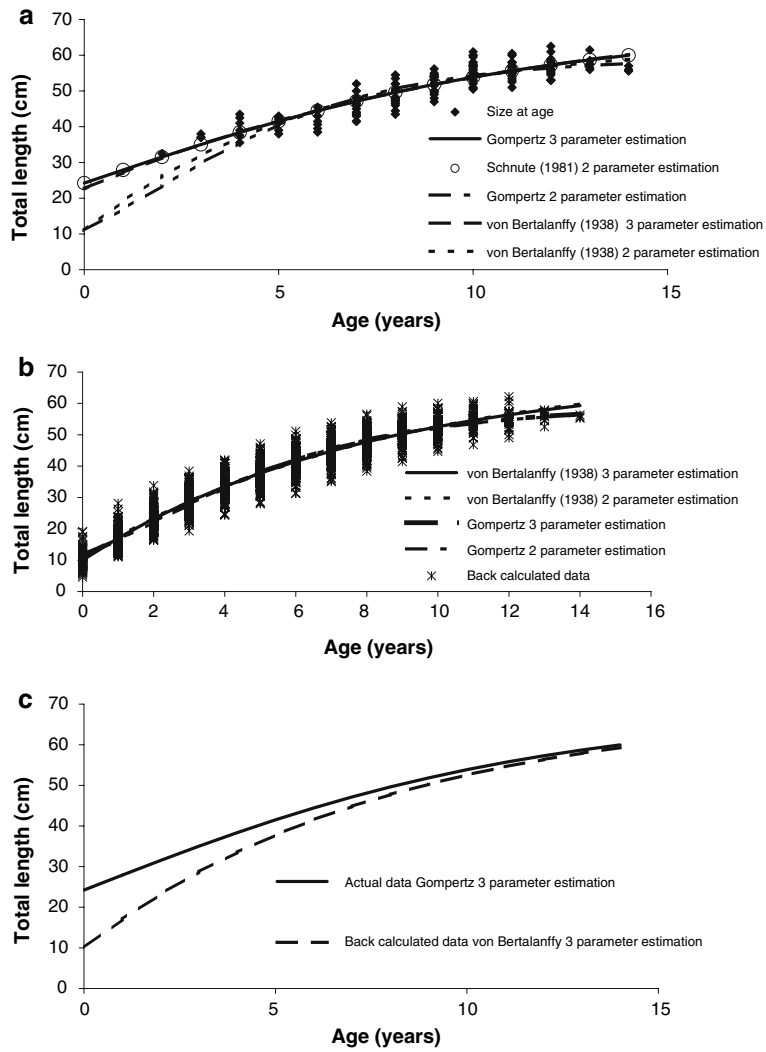

Fig. 6 Female smooth skate growth curves based on (**a**) observed data; (**b**) back-calculated data; and (**c**) observed and back-calculated comparison

Another interesting aspect of female marginal increments concerns the lack of congruency between male and female increment growth. There was a distinct difference in the timing of the peaks between male and female mean MIR. Male marginal increments peaked 3 months earlier and reached numerical lows 2 months earlier than females suggesting a difference in the timing of band deposition of the band pairs. Since skates of all size classes were utilized for MIA, the disparity cannot be resolved due to differences in skate size. Since the reproductive cycles of the sexes are synchronous, it would be unlikely that reproductive events are responsible for the difference in band deposition cycles between the sexes (Sulikowski et al. in press). At this time the size and age at maturity for the smooth skate is unknown, but one possibility is that the females stop depositing band pairs on a regular basis once they are mature. This was directly observed in the little skate, *Raja erinacea*, in a laboratory study where two tetracycline injected females that were laying eggs did not deposit annual bands, whereas the six non-reproductively active females deposited clear band pairs (Natanson 1993). In the event that the mature smooth skate females deposit annual bands sporadically, or not at all, the timing would be unpredictable and the ages as related to size would be less predictable than the males. In fact in this study the females were much more difficult to age as is evidenced by the larger values for CV, APE and D in the females than

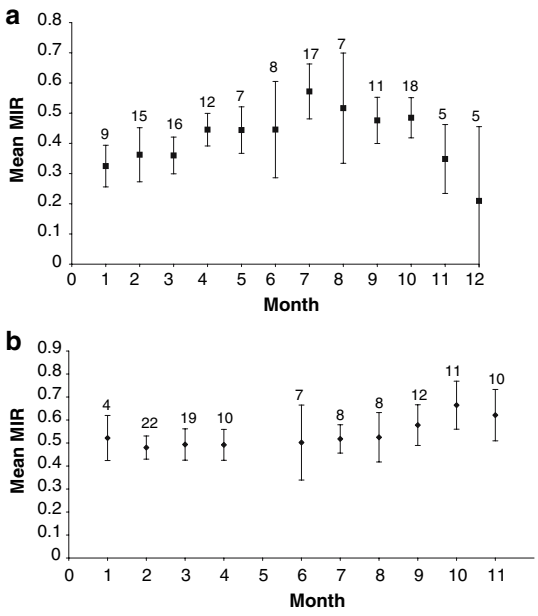

Fig. 7 Mean monthly marginal increments for (**a**) male and (**b**) female smooth skates, *Malacoraja senta.* Sample sizes are given above each corresponding month. Error bars represent 1 ± SD

males and there was greater variability in the observed length at age values. Additionally, the observed data was not as easily fit with a growth model.

Male and female growth diverged at both ends of the data range and thus the sexes required different growth functions to best describe them. While the fitting of growth models to the male smooth skate data was fairly straightforward, the fitting of models to the female data was challenging. The typical growth curve of the observed male data was able to be fit using a variety of models with the main difference being in the size at birth estimation. All of the models, which estimated all parameters, overestimated size at birth. Setting the size at birth and using the VBGF provides the best fit though in fact the curves for all of the models fit that data similarly past age three to four (Fig. 5a). The lack of individuals less than 6 years old is the most likely reason for the inability of the curve to adequately represent the birth size. The lack of small individuals for this study is cause for the use of back-calculation. However, the male growth curves produced using back-calculated values were not sufficiently different from those calculated using the observed values. The female observed data was not a typical growth curve and contained a depression at age six and did not completely reach an asymptote (Fig. 6a). This shape along with the lack of small individuals made it difficult for the models to adequately predict female growth. The best fit for the female observed data was the GGF 3 parameter estimation, though even that overestimated size at birth (Table 3). Despite the different growth parameters the curves for all of the models overlapped past age four; the difference before age four being a result of setting the size at birth on the two parameter estimations. In the case of the female data the use of the back-calculated data vastly improved the fit of all growth models and the traditional 3 parameter VBGF provided the best fit to these data. The difficulty in fitting VBGFs is not unprecedented in elasmobranchs in fact over estimation of the size at birth is quite common (Carlson et al. 2003; Bishop et al. 2006; Natanson et al. in press). The recent use of set sizes at birth indicates that this is problem needs to be addressed. Often as is probably the case in this study, the growth functions have difficulty due to low sample sizes in the younger ages. Additionally, the VBGF has difficulty with species that have rapid initial growth this had lead to the introduction of the use of different growth models to describe growth (Bishop et al. 2006; Natanson et al. 2006).

Females of other elasmobranch species have also been shown to have growth that is less easily defined than the males. Several studies on the shortfin mako, *Isurus oxyrinchus*, had similar findings with females such as no asymptote and high estimates of size at birth from their von Bertalanffy (1938) equation and felt that the Schnute (1981) four parameter function (Bishop et al. 2006) or the GGF 3 parameter model (Natanson et al. 2006) better described growth. While this is a very unrelated species, it is possible that the reproductive energy demands placed on females of a viviparous species with large young causes the female to divert calcium from the

Table 5 Comparison of von Bertalanffy growth parameters for several similar sized skate species

Scientific name	Sex	L_∞ (mm)	k	Max age (yr)	Source
Raja erinacea	♀♂	527 (TL)	0.35	8	Waring 1984
Raja wallacei	♀♂	422 (DW)	0.26	15	Walmsley-Hart et al. 1999
Raja montagui	♂	687 (TL)	0.19		Holden 1972
Raja montagui	♀	728 (TL)	0.18		Holden 1972
Malocoraja senta	♂	754 (TL)	0.12	15	This study
Malocoraja senta	♀	696 (TL)	0.12	14	This Study

DW = Disk width; TL = Total length

structural components to the young. This phenomenon needs further investigation before any conclusions can be drawn. The lack of comparison to other similar species also precludes a definitive answer at this time.

Growth rates and oldest aged specimens were similar for both sexes of smooth skates (k = 0.12; age = 14 for females and k = 0.12, age = 15 for males). These data are in agreement with the life history values from similar sized skates species (Table 5). For instance, the Antarctic skate *Amblyraja georgiana*, which reaches a total length of 71 cm, has been aged to 13 years and found to have a corresponding k value of 0.31 for combined sexes (Francis and Maolagáin 2005).

The current study of the smooth skate demonstrates the potential value of using alternative growth models to the commonly used VBGF. This is especially important as demographic analyses requires accurate determinations of the growth coefficient if stock assessments are to be successful in preventing overexploitation of a species (e.g., Cortés 1999; Goldman 2002; Neer and Thompson 2005). The basic age and growth parameters for the smooth skate provided in the present study support the hypothesis that *M. senta*, like other elasmobranchs, require conservative management because of their slow growth rate and susceptibility to over-exploitation (Brander 1981; Kusher et al. 1992; Zeiner and Wolf 1993; Frisk et al. 2001; Sulikowski et al. 2003, 2005).

Acknowledgements We would like to extend our appreciation to Malcolm Francis for running our Schnute growth functions and providing invaluable insights into that method. Additionally, both Malcolm and John Carlson provided much appreciated time saving spreadsheets, which made our analysis less painful. We would also like to thank Olivia Marcus for help in processing the histological samples and Joseph Deppen for sealing the slides. We appreciate the help provided by Karen Tougas in formatting this paper and the continued support of all members of the Apex Predators Investigation. This work was supported by New Hampshire Sea Grant Development grant #NA16RG1035.

References

Akaike H (1973) Information theory and the extension of the maximum likelihood principle. In: Petrov BN, Csaki F (eds) International symposium on information theory. Academiai Kaido, Budapest, pp 267–281

Beamish RJ, Fournier DL (1981) A method for comparing the precision of a set of age determinations. Can J Fish Aquat Sci 38:982–983

Bishop SDH, Francis MP, Duffy C, Montgomery JC (2006) Age, growth, maturity, longevity and natural mortality of the shortfin mako (Isurus oxyrinchus) in New Zealand waters. Mar Fresh Res 57:143–154

Bonfil R (1994) Overview of world elasmobranch fisheries. FAO Fisheries Technical Paper No. 341, 119 pp

Bowker AH (1948) A test for symmetry in contingency tables. J Am Stat Assoc 43:572–574

Brander K (1981) Disappearance of common skate Raia batis from Irish Sea. Nature 290:48–49

Cailliet GM, Martin LK, Kusher D, Wolf P, Welden BA (1983) Techniques for enhancing vertebral bands in age estimation of California elasmobranchs. In: Prince ED, Pulos LM (eds) Proceedings International Workshop on Age Determination of Oceanic Pelagic Fishes: Tunas, Billfishes, Sharks, NOAA Tech Rep NMFS 8:157-165

Campana SE, Annand MC, McMillan JI (1995) Graphical and statistical methods for determining consistency of age determinations. Trans Amer Fish Soc 124:131–138

Carlson JK, Cortés E, Bethea D (2003) Life history and population dynamics of the finetooth shark (Carcharhinus isodon) in the northeastern Gulf of Mexico. Fish Bull 101:281–292

Casey JG, Pratt HL Jr., Stillwell CE (1985) Age and growth of the sandbar shark(Carcharhinus plumbeus) from the western North Atlantic. Can J Fish Aquat Sci 42(5):963–975

Casey JM, Myers RA (1998) Near extinction of a large, widely distributed fish. Science 281:690–692

Chang WYB (1982) A statistical method for evaluating the reproducibility of age determination. Can J Fish Aquat Sci 39:1208–1210

Cortés E (1999) A stochastic stage-based population model of the sandbar shark in the western North Atlantic. In: Musick JA (ed) Ecology and conservation of long-lived marine animals. Amer Fish Soc Symp 23:115–136

Dulvy NK, Reynolds JD (2002) Predicting extinction vulnerability in skates. Conserv Biol 16:440–450

Evans GT, Hoenig JM (1998) Testing and viewing symmetry in contingency tables, with application to readers of fish ages. Biometrics 54:620–629

Francis MP, Ó Maolagáin C (2005) Age and growth of the Antarctic Skate (Amblyraja georgiana) in the Ross Sea. CCAMLR Sci 12:183–194

Frisk MG, Miller TJ, Fogarty MJ (2001) Estimation and analysis of biological parameters in elasmobranch fishes: a comparative life history study. Can J Fish Aquat Sci 58:969–981

Goldman KJ (2002) Aspects of Age, Growth, Demographics and Thermal Biology of Two Lamniform Shark Species. Ph.D. dissertation, College of William and Mary, School of Marine Science, Virginia Institute of Marine Science, 220 pp

Goldman KJ (2004) Age and growth of elasmobranch fishes. In: Management Techniques for Elasmobranch Fisheries. Musick JA, Bonfil R (eds) FAO Fisheries Technical Paper, No. 474. Rome, FAO. 251 p (electronic version available at http://www.flmnh.ufl.edu/fish/organizations/ssg/EFMT2004.htm)

Haddon M (2001) Growth of individuals In: Modelling and quantitative measures in fisheries, Chapman & Hall/CRC Press, Boca Raton, FL, pp 187–246

Hoeing JM, Morgan MJ, Brown CA (1995) Analyzing differences between two age determination methods by tests of symmetry. Can J Fish Aquat Sci 52:364–368

Holden MJ (1972) The growth rates of *Raja brachyura*, *R. clavata* and *R. montagui* as determined from tagging data. J Cons Int Explor Mer 34(2):161–168

Humason GL (1972) Animal tissue techniques, 4th edn. W.H. Freeman and Company, San Francisco, 661 pp

Kimura DE (1980) Likelihood methods for the von Bertalanffy growth curve. Fish Bull 77(4):765–776

Kusher D, Smith SE, Cailliet GM (1992) Validated age and growth of the leopard shark, Triakis semifasciata, with comments on reproduction. Environ Biol Fish 35:187–303

Martin LK, Cailliet GM (1988) Age and growth of the bat ray, Myliobatis californica, off central California. Copeia 1988(3):762–773

McEachran JD (2002) Skates: Family Rajidae. In: Collette B, Klein-MacPhee G (eds) Bigelow and Schroeder's Fishes of the Gulf of Maine, 3rd edn. Smithsonian Institution Press, pp 60–75

McNemar Q (1947) Note on the sampling error of the difference between correlated proportions or percentages. Psychometrika 12:153–157

Musick JA (1999) Ecology and conservation of long-lived marine animals. In: Musick JA (ed) Life in the slow lane: Ecology and conservation of long-lived marine animals. American Fisheries Society Symposium 23:1–10

Musick JA (2004) Introduction: management of sharks and their relatives (Elasmobranchii), pp 1–6. In: Management Techniques for Elasmobranch Fisheries. Musick JA, Bonfil R (eds) FAO Fisheries Technical Paper, No. 474. Rome, FAO. 251 p (electronic version available at http://www.flmnh.ufl.edu/fish/organizations/ssg/EFMT2004.htm)

Natanson LJ (1993) Effect of temperature on band deposition in the little skate, Raja erinacea. Copeia 1993(1):199–206

Natanson LJ, Ardizzone D, Cailliet GM, Wintner S, Mollet H (2006) Validated age and growth estimates for the shortfin mako, Isurus oxyrinchus, in the North Atlantic Ocean. Special volume from symposium of the American Elasmobranch Society, July 2005. Goldman KJ, Carlson JK (eds) Environ Biol Fish 77:367–383

Neer JA, Thompson BA (2005) Life history of the cownose ray, Rhinoptera bonasus, in the northern Gulf of Mexico, with comments on geographic variability in life history traits. Environ Biol Fish 73:321–331

New England Fishery Management Council (2001) 2000 Stock Assessment and Fishery Evaluation (SAFE) Report for the Northeast Skate Complex. Newburyport, MA, 179 pp

New England Fishery Management Council (2003) Skate Fisheries Management Plan. 50 Water Street, Mill 2 Newburyport, MA, 01950

Ricker WE (1975) Computations and interpretation of biological statisticsof fish populations. Fish Res Bd Canada Bull 191. 382 pp

Ricker WE (1979) Growth rates and models. In: Hoar WS, Randall DJ, Brett JR (eds) Fish physiology, vol VIII: Bioenergetics and growth. Academic Press, Florida, pp 677–743

Robins CR, Ray GC (1986) A Field Guide to Atlantic Coast Fishes of North America. Houghton Mifflin Company, Boston, USA, 354 pp

Schnute J (1981) A versatile growth model with statistically stable parameters. Can J Fish Aquat Sci 38:1128–1140

Simpfendorfer CA, Chidlow J, McAuley R, Unsworth P (2000). Age and growth of the whiskery shark, Furgaleus macki, from southwestern Australia. Environ Biol Fish 58:335–343

Skomal GB (1990) Age and growth of the blue shark, Prionace glauca, in the North Atlantic. Master's Thesis, University of Rhode Island, 82 pp

Sulikowski JA, Morin MD, Suk SH, Howell WH (2003) Age and growth of the winter skate (Leucoraja ocellata) in the western Gulf of Maine. Fish Bull 101:405–413

Sulikowski JA, Kneebone J, Elzey S, Danley P, Howell WH, Tsang PCW (2005) Age and growth estimates of the thorny skate, Amblyraja radiata, in the Gulf of Maine. Fish Bull 3:161–168

Sulikowski JA, Elzey S, Kneebone J, Howell WH, Tsang PCW (2007) The reproductive cycle of the smooth skate, Malacoraja senta, in the Gulf of Maine. J Mar Fresh Res 58:98–103

Taylor CC (1958) Cod growth and temperature. J Cons Int Explor Mer 23:366–370

von Bertalanffy L (1938) A quantitative theory of organic growth (inquiries on growth laws II). Hum Biol 10:181–213

Walmsley-Hart SA, Sauer WHH, Buxton CD (1999) The biology of the skates Raja wallacei and R. pullopunctata (Batoidea:Rajidae) on the Agulhas Bank, South Africa. S. Afr J Mar Sci 21:165–179

Waring GT (1984) Age, growth, and mortality of the little skate off the northeast coast of the United States. Trans Am Fish Soc 113:314–321

Yoccoz NG (1991) Use, overuse, and misuse of significance tests in evolutionary biology and ecology. Bull Ecol Soc Am 71:106–111

Zeiner SJ, Wolf P (1993) Growth characteristics and estimates of age at maturity of two species of skates (Raja binoculata and Raja rhina) from Monterey Bay, California. NOAA Tech Rep 115:87–99